https://doi.org/10.3311/PPci.21945



**Periodica Polytechnica Civil Engineering,** 67(3), pp. 757–764, 2023

# Effect of Activator Type on Geopolymer Mortars Containing Different Types of Fly Ash

Veysel Akyüncü[1], Yunus Emre Avşar[1*], Tolga Enes Emre[1]

[1] Department of Civil Engineering, Çorlu Engineering Faculty, Tekirdağ Namık Kemal University, 59860 Tekirdağ, Türkiye
[*] Corresponding author, e-mail: yeavsar@nku.edu.tr

Received: 27 January 2023, Accepted: 28 March 2023, Published online: 12 April 2023

**Abstract**

In this study, the influence of the activator type on the physical and mechanical properties of the geopolymer mortars was analyzed. C and F-class fly ash (FA), blast furnace slag (BFS), sodium hydroxide (NH), sodium metasilicate (NS), standard sand, and distilled water were used in the production of mortar specimens. All specimens were cured at room temperature. C and F-class fly ash usage ratios are 0%, 15%, and 30%. NH was used as an activator in the 1st group of the produced geopolymer mortars, and NS with NH was used in the 2nd group. 5 series were produced and a flow-table test, ultrasonic pulse velocity test, flexural strength test, compressive strength test, and Scanning Electron Microscope-Energy Dispersive Spectrometry (SEM-EDS) microstructure analysis were applied to the samples. The addition of NS increased the compressive strength and the greatest increase occurred in the reference sample by 113%. It also increased the compressive strength of FAF30 by 60% in comparison to FAC30. Following the results of the SEM examination, when the reference samples were compared, the addition of NS inhibited the formation of cracks. According to the SEM-EDS analysis results, an increase in the F and C-class FA ratio improved the crack formation. Compared to F-class FA, FAC30 has more cracks due to the lower $SiO_2$ content in C-class FA. High K content and $SiO_2$ ratio, as determined by EDS analysis, boost the alkalinity and positively impact the strength.

**Keywords**

geopolymer, ultrasonic pulse velocity, flexural strength, compressive strength, SEM-EDS

## 1 Introduction

Cement is one of the most consumed materials in the world after water [1], and 4.4 billion tons of cement produced worldwide in 2021 [2]. The amount of carbon dioxide ($CO_2$) emitted during cement production is the material's most significant disadvantage in terms of sustainable and environmentally friendly production. It is estimated that the cement industry accounts for approximately 8% of global $CO_2$ emissions [3]. Geopolymer materials, which are an environmentally friendly alternative to cement [4], are produced by the reaction of aluminosilicate-containing solids (blast furnace slag, fly ash, silica fume, metakaolin, etc.) and alkaline solutions (sodium hydroxide, sodium metasilicate, etc.) [5–33]. Compared to cement, geopolymer has advantages such as reduced environmental pollution, economic contribution through reduced natural resource consumption, and advanced durability properties. In addition, geopolymer provides a denser, compact, and homogeneous structure [4, 6, 7].

Geopolymer properties vary according to chemical composition, binder fineness, activator type, activator quantity, and curing type [8, 9]. One of the most commonly produced mixtures, slag-based systems have high strength and durability. As alkali activators, sodium silicate (NS) and sodium hydroxide (NH) are generally preferred in the production of geopolymers [8, 10–14]. While these activators facilitate the dissolution of the binder material by increasing the pH level, they can lead to issues such as rapid setting, high drying shrinkage, and microcrack formation [15, 16]. Kopecskó et al. [17] determined that the maximum compressive strength of 7 days-mixtures cured at room temperature was 91.7 MPa. Heat curing accelerated the chemical reaction, and had a strength-enhancing effect in all mixtures. The maximum strength achieved by heat curing at the age of 7 days was 110.4 MPa.

**Cite this article as:** Akyüncü V., Avşar Y. E., Emre, T. E. "Effect of Activator Type on Geopolymer Mortars Containing Different Types of Fly Ash", Periodica Polytechnica Civil Engineering, 67(3), pp. 757–764, 2023. https://doi.org/10.3311/PPci.21945

Activator type [7, 18], alkali activator/binder (Al/b) ratio [19, 20], NH molarity [19–23], and NS/NH ratio [19, 20, 24–29] affect the physical and mechanical properties of geopolymers.

Examining the literature reveals that NS and NH are the most frequently used activator combinations [19, 20, 24, 25, 27, 28, 30]. NS is more effective than NH at increasing strength, and the combination of NS and NH results in high strength [7]. It has been reported that the use of NH+NS solution provides greater compressive strength for FA and FA+BFS pastes than the use of NH or NS solution alone. For BFS paste, the presence of silicate enhanced the development of strength, and the NS solution (173 MPa) outperformed the NH+NS solution (171.7 MPa) [18].

It has been reported that decreasing the activator/binder (Al/b) ratio from 0.4 to 0.35 increases the compressive strength. The amount of activator has a more significant effect on compressive strength at an early age [20]. Increasing the Al/BFS ratio from 0.4 to 0.5 decreased the 7-day compressive strength by 17% and the 28-day compressive strength by 14%. While the increase in the Al/BFS ratio (0.4, 0.45, 0.5) increased the porosity, it decreased the compressive strength, modulus of elasticity, and flexural strength at 7 days [19].

The increase in NH molarity ascends the compressive strength. The alkalinity, which causes the Ca-O, Al-O, and Si-O bonds to break in BFS and rises the formation of hydration products, increases the strength [21–23]. Ascending the NH molarity from 10M to 12M raised the compressive strength by about 23% [20]. The increase in NH molarity ascended the compressive strength, flexural strength, modulus of elasticity, and porosity of the BFS-based geopolymer [19].

Another factor affecting the compressive strength is the NS/NH ratio. The increase in the NS/NH ratio increases the compressive strength. This is associated with an increase in NS anions. NS anions react with Ca2+ dissolved from the BFS surface and form a C-S-H gel [26]. In a study investigating the effect of the NS/NH ratio (1.5, 2, 2.5) on compressive strength, it was determined that the effect of the NS/NH ratio varies depending on early and advanced age. While the increase in the NS/NH ratio at an early age increased compressive strength, it decreased it in advanced age [20]. Similar results were observed by Deb et al. [24] and Mijarsh [27]. In a study examining the effect of the NS/NH ratio (0.5, 1.5, 2.5) on the compressive strength of silica fume (SF) and BFS-based geopolymer, it was determined that the increase in NS/NH ratio increased the compressive strength and the optimum NS/NH ratio was 2.5 [25]. The increase in the NS/NH ratio (3.25, 2.5, 1.75) increased the compressive strength, flexural strength, modulus of elasticity, and porosity of the BFS-based geopolymer [19]. High NH concentration in C-class FA-based geopolymers can reduce the compressive strength unlike F-class FA-based geopolymers [29]. When the NS/NH ratio is 1 or 2, the increase in silica modulus ($SiO_2/Na_2O$) decreases the compressive strength, while it increases when the NS/NH ratio is 1.5 or 2.5 [28].

In terms of industrial waste disposal, the utilization of BFS and FA in the production of geopolymers is crucial. This circumstance will strengthen the construction industry's commitment to sustainable production and contribute to the reduction of environmental issues, particularly air pollution. The efficient use of BFS and FA is intended to reduce the strain on natural resources, lower cement consumption, and reduce carbon footprint. This study investigated the effect of activator type on the physical and mechanical properties of BFS and FA-based geopolymer mortars. Utilizing various activator combinations and pozzolans will advance geopolymer technology.

Studies examining the effects of curing types, the use of different activator combinations, or different pozzolans on the physical properties (electrical/thermal conductivity, impermeability, sulfate/corrosion resistance, etc.) of geopolymers can contribute to the advancement of geopolymer technology. These studies are crucial for avoiding environmental issues and fostering sustainable manufacturing in the construction industry.

## 2 Material and methods

### 2.1 Materials and mixing ratios

BFS by ASTM C989 [34], C-class FA, and F-class FA by ASTM C618 [35] obtained from İSDEMİR Iron-Steel Factory, Çayırhan Thermal Power Plant, and Sugözü Thermal Power Plant, respectively were used as binding materials in the production of mortar samples.

F-class FA is produced by burning anthracite or bituminous coal. It has pozzolanic properties. C-class FA is obtained as a result of burning lignite or sub-bituminous coal. In addition to pozzolanic properties, it also has binding properties [35].

NS and NH were used as activators. The chemical and physical properties of BFS and FA are given in Table 1 and Table 2, respectively. The specific gravity and specific surface area of the binder materials were determined by helium pycnometer and Blaine method, respectively.

**Table 1** Chemical properties of BFS and FAs

| Property | Materials | | |
|---|---|---|---|
| | BFS | FA-F | FA-C |
| CaO (by weight, %) | 35.26 | 1.54 | 13.2 |
| $SiO_2$ (by weight, %) | 40.07 | 62 | 49.13 |
| $Al_2O_3$ (by weight, %) | 12.16 | 20.41 | 15.04 |
| $Fe_2O_3$ (by weight, %) | 0.77 | 7.35 | 8.25 |
| S + A + F | - | 89.76 | 72.42 |
| $SO_3$ (by weight, %) | 0.17 | 0.16 | 3.84 |
| MgO (by weight, %) | 6.73 | 1.78 | 4.76 |
| Total Alkalies ($Na_2O + 0.658*K_2O$) (by weight, %) | 0.8 | 2.55 | 3.96 |
| $Na_2O$ | - | 1.19 | 2.2 |
| $Cl^-$ (ppm) | 50 | 10 | - |

**Table 2** Physical properties of BFS and FAs

| Property | Materials | | |
|---|---|---|---|
| | BFS | FA-F | FA-C |
| Insoluble Residue (by weight, %) | 0.66 | 0.87 | - |
| Loss of Ignition (by weight, %) | 0.78 | 2.05 | 0.72 |
| Specific Gravity | 2.92 | 2.21 | 2.34 |
| Specific Surface ($cm^2/g$) | 3880 | 2780 | 2100 |

Fig. 1 shows the F-class FA and SEM images used in the study. The FA particles are observed to have a spherical structure. Fig. 2 shows the BFS and SEM images used in the study. The BFS particles are observed to have an angular structure.

CEN reference sand conforming to TS EN 196-1 [36] was used in the production of the mortar samples. CEN reference sand is natural sand containing a high amount of $SiO_2$ (at least 98%) and has isometric and rounded particles [36]. The density of CEN reference sand is roughly 2.6 $g/cm^3$. Sieve analysis of CEN reference sand is given in Table 3. The properties of NH and NS are given in Table 4.

### 2.2 Methods

Thirty mortar samples (40 × 40 × 160 mm) were made for the experiment according to the TS EN 196-1 [36]. FA was utilized by substituting 0%, 15%, and 30% of BFS by weight. Five mortar series were manufactured. In the first group of each mortar series, NH was used as the activator, while NH+NS was used in the second group. Following 28 days, tests were conducted on the samples.

900 gr binder was used in the production of the mortar series. The sand/binder ratio is 3, the NH molarity is 10M, and the use of plasticizer additives is 1.2% by weight of the binder. The codes and the usage ratios of the materials are

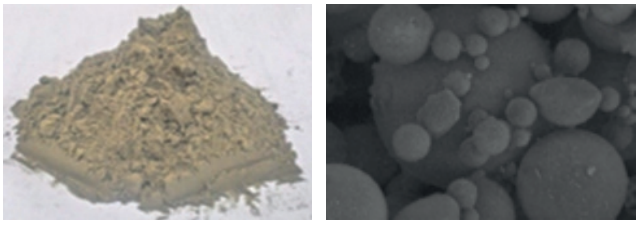

(a) (b)

**Fig. 1** F-class FA (a) and SEM image (b)

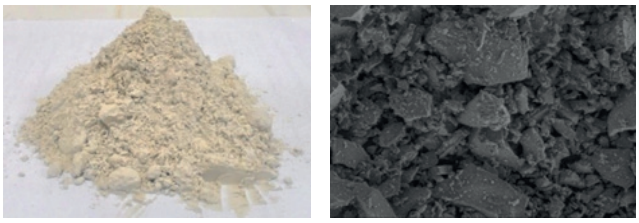

(a) (b)

**Fig. 2** BFS (a) and SEM image (b)

**Table 3** Sieve analysis of CEN reference sand

| Sieve analysis of CEN reference sand | |
|---|---|
| Square Mesh (mm) | Cumulative Sieve Residue (%) |
| 2 | 0 |
| 1.6 | 7 ± 5 |
| 1 | 33 ± 5 |
| 0.5 | 67 ± 5 |
| 0.16 | 87 ± 5 |
| 0.08 | 99 ± 5 |
| 2 | 0 |

**Table 4** Properties of NH and NS

| Chemical composition of NH | |
|---|---|
| Property | Value |
| Molecular Weight | 40 g/mol |
| $Na_2CO_3$ | ≤1 |
| Cl | <0,01 |
| SO4 | ≤0,01 |
| Purity | %99 |
| **Chemical and physical properties of NS** | |
| Property | Value |
| $Na_2O$ (%) | 28.1–29.5 |
| $SiO_2$ (%) | 28–29.4 |
| Solid Content (%) | 57.5 |
| Silica Module | 1.01–1.05 |
| Weight Ratio | 0.98–1.02 |
| Density ($g/cm^3$) | 0.85–1.05 |
| pH | 12–13 |
| Melting Temperature (°C) | 72 |
| Color | White |
| Particle Type | Granular |

given in Table 5 (NS: Sodium metasilicate; NH: Sodium hydroxide; B: Binder; NS S: Sodium metasilicate Solution; NH S: Sodium hydroxide Solution; NS W: Sodium metasilicate Water; Ref: Reference). The reference mortar series represents 100% BFS-substituted mortar samples. Water/binder and solution/binder ratios are 0.5 and 0.4, respectively. Plasticizer usage ratio, NS S/NH S, and NS W/NS S values were determined as a result of preliminary studies.

Flow-table test by TS EN 1015-3 [37], ultrasonic pulse velocity test by TS EN 12504-4 [38], flexural and compressive strength test by TS EN 196-1 [36] were performed on the mortar samples.

## 3 Results and discussions

Fig. 3 displays the flow-table values for the mortar series.

Fresh mortar was placed in the cone by tamping 10 times with the rod in two stages. The diameters of the fresh mortar were measured after 15 falls for 60 seconds. The average of the diameters of the spread mortar in the x and y-axis directions was calculated.

The flow-table value of fresh mortars made with NH ranges from 108 to 117 mm, whereas the flow-table value of fresh mortars made with NH+NS ranges from 110 to 125 mm. The addition of NS improved the flow-table value (except FAC30 and FAF15). Observations revealed that the usage ratio and type of FA did not significantly affect the flow-table value.

Table 6 contains the test findings acquired for the mortar series. The test results for ultrasonic pulse velocity, flexural and compressive strength are depicted in Figs. 4, 5, and 6, respectively.

**Table 5** Codes and experimental design

| Groups | Series | FA (%) | BFS (%) | NS S/NH S | NS W/NS S |
|---|---|---|---|---|---|
| NH | Ref | 0 | 100 | - | - |
| | FAC15 | 15 | 85 | | |
| | FAC30 | 30 | 70 | | |
| | FAF15 | 15 | 85 | | |
| | FAF30 | 30 | 70 | | |
| NH+NS | Ref | 0 | 100 | 1.88 | 0.6 |
| | FAC15 | 15 | 85 | | |
| | FAC30 | 30 | 70 | | |
| | FAF15 | 15 | 85 | | |
| | FAF30 | 30 | 70 | | |

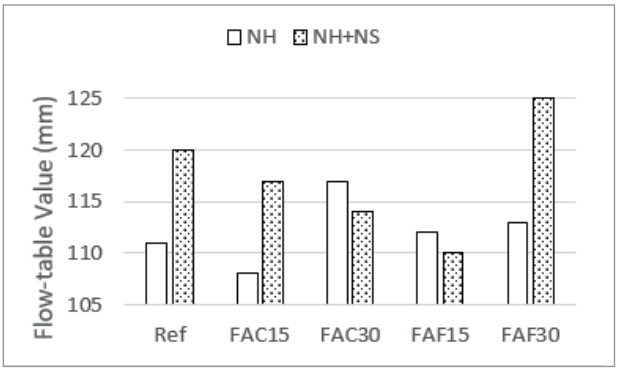


**Fig. 3** Flow-table test results

**Table 6** Test results

| Codes | | UPV | Flexural Strength | Compressive Strength |
|---|---|---|---|---|
| Groups | Series | km/s | MPa | MPa |
| NH | Ref | 4.238 | 6.2 | 22.5 |
| | FAC15 | 3.943 | 5.1 | 25.5 |
| | FAC30 | 3.898 | 5.0 | 21.0 |
| | FAF15 | 3.942 | 5.8 | 30.1 |
| | FAF30 | 3.637 | 4.7 | 19.8 |
| NH+NS | Ref | 4.267 | 6.2 | 47.9 |
| | FAC15 | 4.150 | 5.5 | 32.8 |
| | FAC30 | 4.046 | 5.2 | 25.6 |
| | FAF15 | 4.040 | 5.4 | 27.8 |
| | FAF30 | 4.030 | 5.0 | 39.7 |

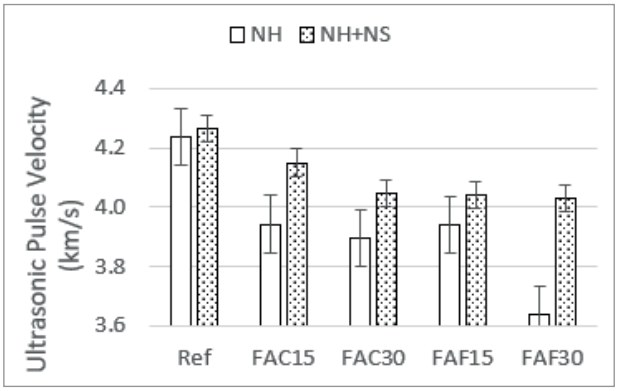


**Fig. 4** Ultrasonic pulse velocity test results

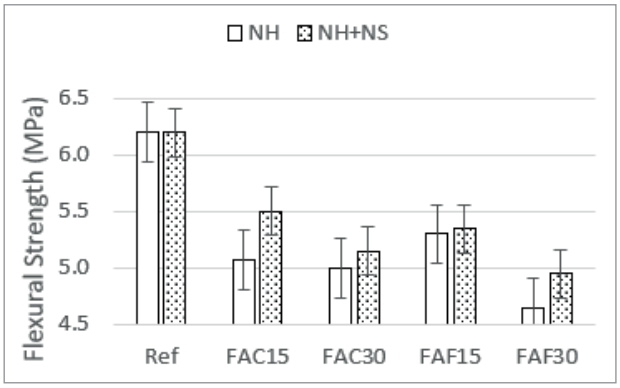


**Fig. 5** Flexural strength test results

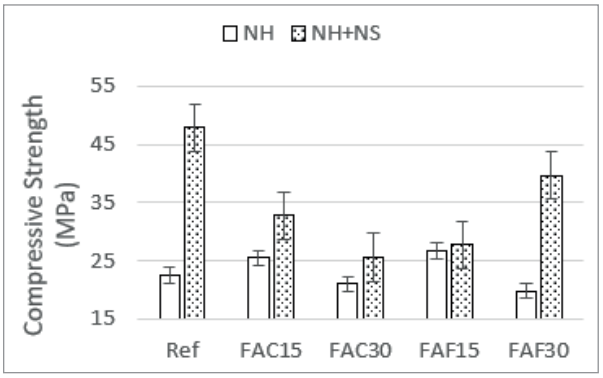


**Fig. 6** Compressive strength test results

In the use of NH, the increase in C and F-class FA decreased the ultrasonic pulse velocity. It appears that the rate of reduction of ultrasonic pulse velocity is higher for the F-class FA substitution. In the use of NH+NS, the increase in C-class FA reduced the ultrasonic pulse velocity by up to 5%. 15% F-class FA substitution reduced the ultrasonic pulse velocity by 5%, while more than 15% did not cause any significant change. The addition of NS increased the ultrasonic pulse velocity in all series. This indicates that NS forms a denser structure by reducing porosity. The greatest increase (10%) occurred in FAF30 (Fig. 4).

In the use of NH, the increase in C and F-class FA reduced the flexural strength by 19% and 24%, respectively, and by 16% and 19% in the use of NH+NS. The addition of NS increased flexural strength (except Ref). It is known that there is a shrinkage problem in geopolymers [39]. Drying shrinkage played an important role in the reduction of flexural strength in the Ref due to microcrack formation [40]. The shrinkage problem may have neutralized the increasing trend in flexural strength caused by the addition of NS in the Ref. In addition, the effect of shrinkage on the flexural strength may have decreased as the FA was added. The greatest increase (8%) occurred in FAC15 (Fig. 5).

15% substitution of C and F-class FA with NH increased the compressive strength by 13% and 33%, respectively. This can be explained by the F-class's greater pozzolanic activity as a result of its higher $SiO_2$ content. The 30% substitution did not significantly alter the situation. The addition of NS increased the compressive strength, and the reference sample (BFS100) showed the greatest increase (113%). This can be explained by the high CaO concentration of BFS, which gives it greater hydraulic binding properties. In addition, the increase in strength owing to the inclusion of NS is a result of the siliceous structure of NS, which increases its pozzolanic property. Phoo-ngernkham et al. [18] discovered that the compressive strength of the (NH+NS)-activated FA-based geopolymer (45 MPa) was 800% greater than the compressive strength of the NH-activated FA-based geopolymer (2.5 MPa). Substituting 15% C- and F-class FA in NH+NS decreased the compressive strength by 31.5% and 42%, respectively. This can be explained by the high CaO content of C-class FA, which increases its hydraulic binding properties. Substitution of 30% C- and F-class FA decreased the compressive strength by 46.5% and 17%, respectively. This can be explained by the F-class's pozzolanic activity as a result of its higher $SiO_2$ content. Therefore, it is evident that hydraulic binding plays an important role at low substitution rates, but pozzolanic activity plays an important role at high substitution rates (Fig. 6).

When the SEM images of the geopolymerization formations are examined, silica crystals, microcracks, porous structure, geopolymer gel, N-A-S-H gel, C-A-S-H gel, BFS, and FA are seen. FA particles have a spherical shape while BFS particles have a sharp angular shape. While silica crystals form at the beginning of the reaction on the FA surface, the silica crystals turn into N-A-S-H gels later on. As a result of the reaction on the BFS surface, a C-A-S-H gel is formed (Fig. 7).

Fig. 8 depicts SEM images of the Ref-NH and Ref-NHNS series. As a result of its siliceous nature, the inclusion of NS considerably reduced crack formation (Fig. 8(b)). This also explains why the addition of NS increased the compressive strength of reference samples (BFS100) by 113%.

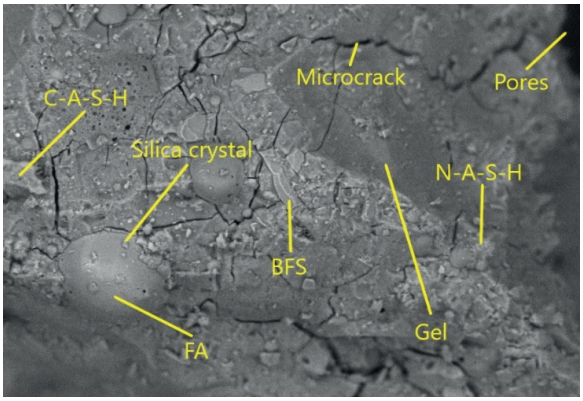


**Fig. 7** Geopolymerization formations

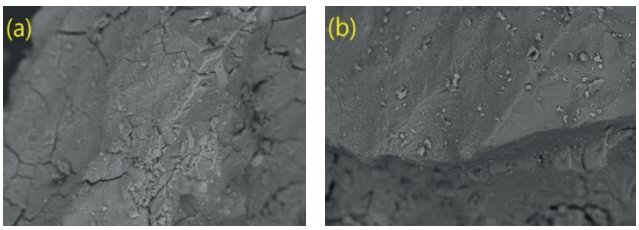


**Fig. 8** SEM images of Ref-NH (a) and Ref-NHNS (b)

Fig. 9 shows the SEM-EDS analysis results of Ref-NHNS, FAC30-NHNS, and FAF30-NHNS. Crack formation is rarely encountered in Ref (47.9 MPa) as BFS has hydraulic binding properties due to its high CaO content. The high CaO content of BFS and the siliceous structure of NS provided a denser C-A-S-H gel formation (Fig. 9(a)). Similar results were obtained by Phoongernkham et al [18]. It was determined that the NH+NS solution geopolymer matrix was denser than the NH solution geopolymer matrix, the fracture surface had fewer unreacted FA particles, and the increased Ca content increased the formation of C-S-H/C-A-S-H with geopolymerization [18]. However, an increase in crack formation was observed with an increase in the F and C-class FA ratio. This is due to the decrease in the amount of CaO. The cracks in the FAC30 (25.6 MPa) series are more numerous than those in the FAF30 (39.7 MPa) series. This is due to the lower SiO2 content in C-class FA compared to F-class FA (Fig. 9(b)). Although the FAF30 series has a high $SiO_2$ content, it contains very low CaO. Therefore, it has a lower compressive strength of about 8 MPa than the Ref series (Fig. 9(c)). 15% F and C-class FA significantly affect the physical/mechanical properties. However, when SEM images were examined, no comparable difference was observed in these series.

Table 7 displays the EDS results for Ref-NHNS, FAC30-NHNS, and FAF30-NHNS. According to the results of EDS, a high K content and SiO2 ratio improve the alkalinity and positively impact the strength.

**Table 7** EDS results of Ref-NHNS, FAC30-NHNS, and FAF30-NHNS

| Codes | Chemical component (%) | | | | | |
|---|---|---|---|---|---|---|
| | Si | Ca | Mg | Al | Na | K |
| Ref-NHNS | 13.1 | 30.9 | 1.2 | 3.4 | 4.9 | 0.9 |
| FAC30-NHNS | 16.1 | 18.3 | 3.9 | 4.3 | 5.7 | 0.8 |
| FAF30-NHNS | 28.4 | 7.1 | 0 | 9.7 | 1 | 15.8 |

## 4 Conclusions

This study investigated the effect of activator type on the physical and mechanical properties of blast furnace slag (BFS) and F and C-class fly ash (FA) based geopolymer mortars.

The addition of NS increased the compressive strength compared to the use of NH alone, with the largest increases (113%) occurring in the control sample (BFS100). This can be explained by the high CaO concentration of BFS, which gives it greater hydraulic binding properties. The rise in compressive strength is attributed to the siliceous structure of NS, which increases its pozzolanic property.

The optimal compressive strength was reached by substituting 30% F-class FA by comparison with C-class FA since F-class FA has greater pozzolanic activity than C-class FA because of F-class FA's higher $SiO_2$ concentration.

Following the results of the SEM examination, when the reference samples were compared, the addition of NS inhibited the formation of cracks because the siliceous structure of NS produced a denser C-A-S-H gel. This explains why the addition of NS resulted in a 113% increase in compressive strength in the reference samples (BFS100).

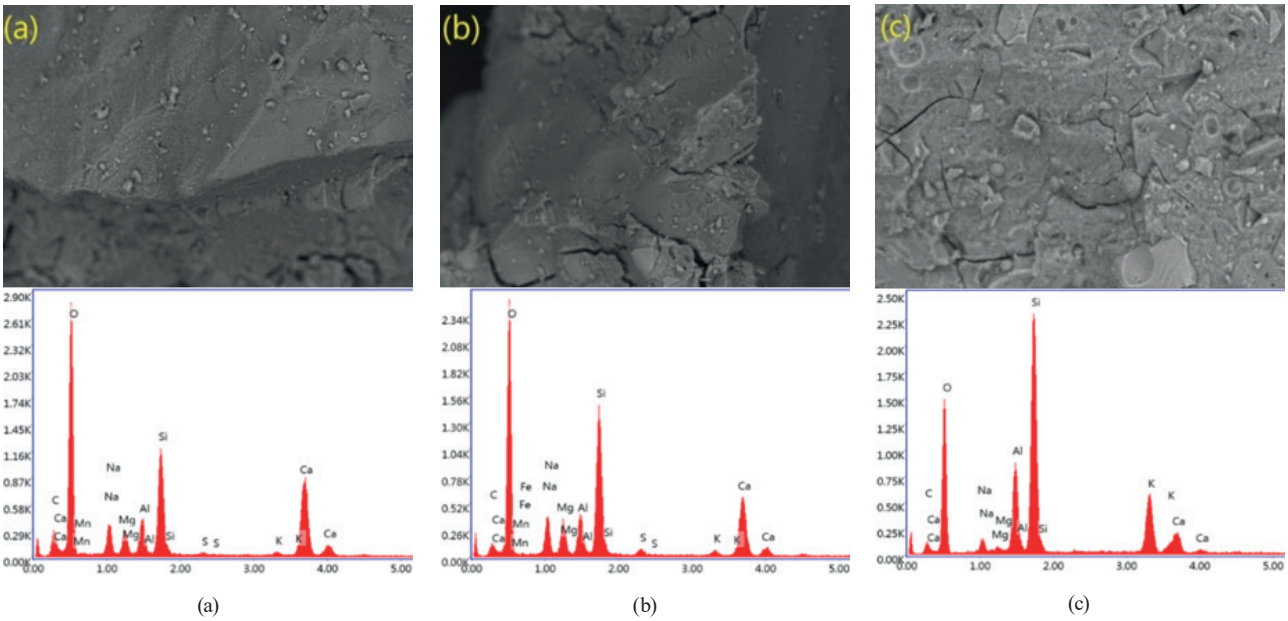


(a) (b) (c)

**Fig. 9** SEM-EDS results of Ref-NHNS (a), FAC30-NHNS (b), and FAF30-NHNS (c)

According to the SEM-EDS analysis results, the decrease in the amount of CaO as a result of the increase in the F and C-class FA ratio increased the crack formation. Compared to F-class FA, FAC30 has more cracks due to the lower $SiO_2$ content in C-class FA. Although FAF30 has a high $SiO_2$ content, it has 17% lower compressive strength than Ref because it contains very low CaO. High K content and $SiO_2$ ratio, as determined by EDS analysis, boost the alkalinity and positively impact the strength.

## References

[1] Gencel, O., Karadag, O., Oren, O. H., Bilir, T. "Steel slag and its applications in cement and concrete technology: A review", Construction and Building Materials, 283, 122783, 2021. https://doi.org/10.1016/j.conbuildmat.2021.122783

[2] USGS "Mineral commodity summaries 2022", U.S. Geological Survey, Reston, VA, USA, 2022. ISBN: 978-1-4113-4434-1 https://doi.org/10.3133/mcs2022

[3] Preston, F., Lehne, J. "Making concrete change innovation in low-carbon cement and concrete", Chatham House - The Royal Institute of International Affairs, United Kingdom, 2018. ISBN: 9781784132729

[4] Alanazi, H., Hu, J., Kim, Y.-R. "Effect of slag, silica fume, and metakaolin on properties and performance of alkali-activated fly ash cured at ambient temperature", Construction and Building Materials, 197, pp. 747–756, 2019. https://doi.org/10.1016/j.conbuildmat.2018.11.172

[5] Rodrigue, A., Duchesne, J., Fournier, B., Bissonnette, B. "Influence of added water and fly ash content on the characteristics, properties and early-age cracking sensitivity of alkali-activated slag/fly ash concrete cured at ambient temperature", Construction and Building Materials, 171, pp. 929–941, 2018. https://doi.org/10.1016/j.conbuildmat.2018.03.176

[6] Güler, G., Güler, E., İpekoğlu, Ü., Mordoğan, H. "Uçucu küllerin özellikleri ve kullanım alanları" (Properties and utilization areas of fly ashes), In: 19th International Mining Congress and Exhibition, İzmir, Türkiye, 2005, pp. 419–423. (in Türkish)

[7] Yazdi, M. A., Liebscher, M., Hempel, S., Yang, J., Mechtcherine, V. "Correlation of microstructural and mechanical properties of geopolymers produced from fly ash and slag at room temperature", Construction and Building Materials, 191, pp. 330–341, 2018. https://doi.org/10.1016/j.conbuildmat.2018.10.037

[8] Duxson, P., Fernández-Jiménez, A., Provis, J. L., Lukey, G. C., Palomo, A., van Deventer, J. S. J. "Geopolymer technology: The current state of the art", Journal of Materials Science, 42(9), pp. 2917–2933, 2007. https://doi.org/10.1007/s10853-006-0637-z

[9] Abdalqader, A. F., Jin, F., Al-Tabbaa, A. "Development of greener alkali-activated cement: utilisation of sodium carbonate for activating slag and fly ash mixtures", Journal of Cleaner Production, 113, pp. 66–75, 2016. https://doi.org/10.1016/j.jclepro.2015.12.010

[10] Palomo, A., Grutzeck, M. W., Blanco, M. T. "Alkali-activated fly ashes: A cement for the future", Cement and Concrete Research, 29(8), pp. 1323–1329, 1999. https://doi.org/10.1016/S0008-8846(98)00243-9

[11] Davidovits, J. "Geopolymers: Inorganic polymeric new materials", Journal of Thermal Analysis and Calorimetry, 37, pp. 1633–1656, 1991. https://doi.org/10.1007/BF01912193

[12] Barbosa, V. F. F., MacKenzie, K. J. D. "Thermal behaviour of inorganic geopolymers and composites derived from sodium polysialate", Materials Research Bulletin, 38(2), pp. 319–331, 2003. https://doi.org/10.1016/S0025-5408(02)01022-X

[13] Xu, H., van Deventer, J. S. J. "The geopolymerisation of alumino-silicate minerals", International Journal of Mineral Processing, 59(3), pp. 247–266, 2000. https://doi.org/10.1016/S0301-7516(99)00074-5

[14] Hardjito, D., Wallah, S. E., Sumajouw, D. M. J., Rangan, B. V. "On the development of fly ash-based geopolymer concrete", ACI Materials Journal, 101(6), pp. 467–472, 2004. https://doi.org/10.14359/13485

[15] Lee, N. K., Lee, H. K. "Setting and mechanical properties of alkali-activated fly ash/slag concrete manufactured at room temperature", Construction and Building Materials, 47, pp. 1201–1209, 2013. https://doi.org/10.1016/j.conbuildmat.2013.05.107

[16] Yuan, X., Chen, W., Lu, Z., Chen, H. "Shrinkage compensation of alkali-activated slag concrete and microstructural analysis", Construction and Building Materials, 66, pp. 422–428, 2014. https://doi.org/10.1016/j.conbuildmat.2014.05.085

[17] Kopecskó, K., Hajdu, M., Balázs, G. L. "Alkali-activated binders based on fly ash and GGBS", In: Proceedings of the 2019 fib Symposium: Concrete Innovations in Materials, Design and Structures, Krakow, Poland, 2019, pp. 2167–2174. ISBN: 9782940643004

[18] Phoo-ngernkham, T., Hanjitsuwan, S., Damrongwiriyanupap, N., Chindaprasirt, P. "Effect of sodium hydroxide and sodium silicate solutions on strengths of alkali activated high calcium fly ash containing Portland cement", KSCE Journal of Civil Engineering, 21(6), pp. 2202–2210, 2017. https://doi.org/10.1007/s12205-016-0327-6

[19] Aliabdo, A. A., Abd Elmoaty, A. E. M., Emam, M. A. "Factors affecting the mechanical properties of alkali activated ground granulated blast furnace slag concrete", Construction and Building Materials, 197, pp. 339–355, 2019. https://doi.org/10.1016/j.conbuildmat.2018.11.086

[20] Fang, G., Ho, W. K., Tu, W., Zhang, M. "Workability and mechanical properties of alkali-activated fly ash-slag concrete cured at ambient temperature", Construction and Building Materials, 172, pp. 476–487, 2018. https://doi.org/10.1016/j.conbuildmat.2018.04.008

[21] Manjunath, G. S., Radhakrishna, Giridhar, C., Jadhav, M. "Compressive strength development in ambient cured geopolymer mortar", International Journal of Earth Sciences and Engineering, 4(6), pp. 830–834, 2011. [online] Available at: https://bit.ly/3kDCcF3 [Accessed: 27.10.2022]

[22] García-Lodeiro, I., Fernández-Jiménez, A., Palomo, A. "Variation in hybrid cements over time. Alkaline activation of fly ash–portland cement blends", Cement and Concrete Research, 52, pp. 112–122, 2013. https://doi.org/10.1016/j.cemconres.2013.03.022

[23] Ryu, G. S., Lee, Y. B., Koh, K. T., Chung, Y. S. "The mechanical properties of fly ash-based geopolymer concrete with alkaline activators", Construction and Building Materials, 47, pp. 409–418, 2013. https://doi.org/10.1016/j.conbuildmat.2013.05.069

[24] Deb, P. S., Nath, P., Sarker, P. K. "The effects of ground granulated blast-furnace slag blending with fly ash and activator content on the workability and strength properties of geopolymer concrete cured at ambient temperature", Materials and Design, 62, pp. 32–39, 2014. https://doi.org/10.1016/j.matdes.2014.05.001

[25] Gupta, A. "Investigation of the strength of ground granulated blast furnace slag based geopolymer composite with silica fume", Materials Today: Proceedings, 44, pp. 23–28, 2021. https://doi.org/10.1016/j.matpr.2020.06.010

[26] Huang, X., Yu, L., Li, D. W., Shiau, Y. C., Li, S., Liu, K. X. "Preparation and properties of geopolymer from blast furnace slag", Materials Research Innovations, 19(10), pp. S10–413-S10-419, 2015. https://doi.org/10.1179/1432891715Z.0000000002210

[27] Mijarsh, M. J. A., Megat Johari, M. A., Ahmad, Z. A. "Effect of delay time and Na2SiO3 concentrations on compressive strength development of geopolymer mortar synthesized from TPOFA", Construction and Building Materials, 86, pp. 64–74, 2015. https://doi.org/10.1016/j.conbuildmat.2015.03.078

[28] Thaarrini, J., Ramasamy, V. "Feasibility studies on compressive strength of ground coal ash geopolymer mortar", Periodica Polytechnica Civil Engineering, 59(3), pp. 373–379, 2015. https://doi.org/10.3311/PPci.7696

[29] Malkawi, A. B., Nuruddin, M. F., Fauzi, A., Almattarneh, H., Mohammed, B. S. "Effects of alkaline solution on properties of the HCFA geopolymer mortars", Procedia Engineering, 148, pp. 710–717, 2016. https://doi.org/10.1016/j.proeng.2016.06.581

[30] Akyüncü, V., Avşar, Y. E. "Physical and mechanical properties of alkali activated mortars produced using different types of fly ash", European Journal of Engineering and Applied Sciences, 5(1), pp. 16–21, 2022. https://doi.org/10.55581/ejeas.1125144

[31] Oderji, S. Y., Chen, B., Ahmad, M. R., Shah, S. F. A. "Fresh and hardened properties of one-part fly ash-based geopolymer binders cured at room temperature: Effect of slag and alkali activators", Journal of Cleaner Production, 225, pp. 1–10, 2019. https://doi.org/10.1016/j.jclepro.2019.03.290

[32] Ravitheja, A., Kumar, N. L. N. K. "A study on the effect of nano clay and GGBS on the strength properties of fly ash based geopolymers", Materials Today: Proceedings, 19, pp. 273–276, 2019. https://doi.org/10.1016/j.matpr.2019.06.761

[33] Bouaissi, A., Li, L., Al Bakri Abdullah, M. M., Bui, Q.-B. "Mechanical properties and microstructure analysis of FA-GGBS HMNS based geopolymer concrete", Construction and Building Materials, 210, pp. 198–209, 2019. https://doi.org/10.1016/j.conbuildmat.2019.03.202

[34] ASTM International "ASTM C989/C989M-22 Standard specification for slag cement for use in concrete and mortars", ASTM International, West Conshohocken, PA, USA, 2022. https://doi.org/10.1520/C0989_C0989M-22

[35] ASTM International "ASTM C618-22 Standard specification for coal fly ash and raw or calcined natural pozzolan for use in concrete", ASTM International, West Conshohocken, PA, USA, 2019. https://doi.org/ 10.1520/C0618-22

[36] TSE "TS EN 196-1 Methods of testing cement-Part 1: Determination of strength", TSE, Ankara, Türkiye, 2016.

[37] TSE "TS EN 1015-3 Methods of test for mortar for masonry-Part 3: Determination of consistence of fresh mortar (by flow table)", TSE, Ankara, Türkiye, 2000.

[38] TSE "TS EN 12504-4 Testing concrete-Part 4: Determination of ultrasonic pulse", TSE, Ankara, Türkiye, 2021.

[39] Frasson, B. J., Rocha, J. C. "Drying shrinkage behavior of geopolymer mortar based on kaolinitic coal gangue", Case Studies in Construction Materials, 18, e01957, 2023. https://doi.org/10.1016/j.cscm.2023.e01957

[40] Jeon, I. K., Ryou, J. S., Jakhrani, S. H., Kim, H. G. "Effects of light-burnt dolomite incorporation on the setting, strength, and drying shrinkage of one-part alkali-activated slag cement", Materials, 12(18), 2874, 2019. https://doi.org/10.3390/ma12182874